Electrochemical Adsorption of OH on Pt(111) in Alkaline Solutions: Combining DFT and Molecular Dynamics

Leandro M. C. Pinto,[a] Paola Quaino,[b] Mauricio D. Arce,[b] Elizabeth Santos,[a, c] and Wolfgang Schmickler*[a]

The adsorption of OH on Pt(111) in alkaline solution has been investigated by a method that combines density functional theory, molecular dynamics, and quantum statistical mechanics. In particular, we have calculated the free energy surface for the reaction. A physisorbed hydroxide ion in a metastable state and a stable adsorbed uncharged OH group are observed. The energy of activation at equilibrium is comparatively low, so that the reaction is fast.

1. Introduction

The adsorption or desorption of OH plays an important role in several fuel cell reactions, especially in alkaline solutions. Thus, OH desorption has been suggested as a reaction step in oxygen reduction (for a review, see ref. [1]); adsorbed OH can act as a bystander that blocks surface sites, and recently it has been proposed that the recombination of adsorbed hydrogen with OH to form water is an important step in hydrogen oxidation in alkaline media.[2] Clearly, elucidating the kinetics of OH adsorption/desorption from an atomistic point of view is necessary for understanding the operation of fuel cells.

Herein, we focus on the adsorption of OH on Pt(111) at low coverage, but our method should work just as well for other metals. This reaction has been investigated by a number of groups—see refs. [3–6] and further references therein. However, these previous studies were based solely on density functional theory (DFT), which can provide the thermodynamics of electrochemical reactions but not their energies of activation. Since the development of early theories of electrochemical reactions, such as proposed by Marcus,[7] Hush,[8] and the Soviet school,[9] it is well known that the solvation of the reactants and in particular solvent fluctuations play a crucial part in the kinetics. Indeed, for outer-sphere electron transfer, during which the reactants are not adsorbed, the influence of the solvent is the dominating effect, since the interaction with the electrode is too weak to affect the energy of activation. However, outer-sphere electron transfer is of limited interest. Because of the world's pressing energy demands we need to understand electrocatalysis, in which at least one of the reactants is adsorbed on the electrode.

For reasons that we have discussed in a recent review[10] and shall not repeat here, we believe that pure DFT is not sufficient to treat the dynamics of electrochemical reactions; therefore we have developed our own approach in our group. We start from a model Hamiltonian that contains the reactants, the electrode, the solvent, and their interactions, and determine the electronic parameters from DFT. In the past, we have applied this theory extensively to hydrogen evolution (see ref. [10] and references therein), and more recently to oxygen reduction.[11] Here we shall apply it to $OH^- \rightarrow OH + e^-$ in alkaline solutions, and use this opportunity to improve the treatment of the solvent substantially. Following ideas that we have developed recently for metal deposition,[12, 13] we have performed molecular dynamics simulations for the reactant in the vicinity of the electrode, and incorporated the results into our framework. We believe that this new procedure is a substantial improvement over our previous preliminary treatment of the same reaction,[10] in which the interaction with the solvent was obtained from estimates based on experimental data.

The rest of this article is organized as follows. We first present the results of DFT calculations for the interaction of the radical OH and the anion OH^- with Pt(111), and show how we obtain the parameters for the electronic interactions. Then we present the result of molecular dynamics simulations and show how the solvation of the anion changes in the vicinity of the electrode surface. Finally, we present the free energy surface for the reaction on the basis of our theory. All technical details have been relegated to the Computational Details.

2. Interaction of OH and OH⁻ with the Pt(111) Surface

During the reaction the OH^- ion approaches the surface, a solvent fluctuation induces electron transfer, and the OH radical is adsorbed. Our model includes the electronic energies of both the initial and final states, their interaction with the solvent,

[a] Dr. L. M. C. Pinto, Dr. E. Santos, Prof. Dr. W. Schmickler
Institute of Theoretical Chemistry, Ulm University
89069 Ulm (Germany)
E-mail: wolfgang.schmickler@uni-ulm.de

[b] Dr. P. Quaino, Dr. M. D. Arce
PRELINE, Universidad Nacional del Litoral
Santa Fe (Argentina)

[c] Dr. E. Santos
Facultad de Matemática, Astronomía y Física
IFEG-CONICET, Universidad Nacional de Córdoba
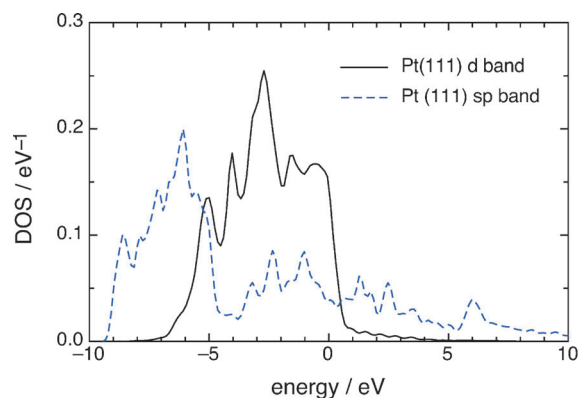Córdoba (Argentina)

and the fluctuations that trigger the transition. To ensure that we have the correct energies for the initial and final states, we need the electronic energies of both OH and OH$^-$ as a function of the distance from the electrode surface. Both can be obtained from DFT; for the radical the calculations are straightforward but for the anion we require a special procedure, which will be presented below.

The isolated OH radical has seven valence electrons and is spin polarized. In a simple description, the O2s orbital mixes with one of the O2p orbitals—in our notation O2p$_{+1}$—and the H1s orbital to form a bonding and an antibonding orbital (see Figure 1). The other two O2p orbitals have the same energy, and share three electrons. In our notation, the O2p$_0$ and O2p$_{-1}$ spin-down orbitals are filled, whereas the corresponding spin-up orbitals lie at the Fermi level and are half filled.
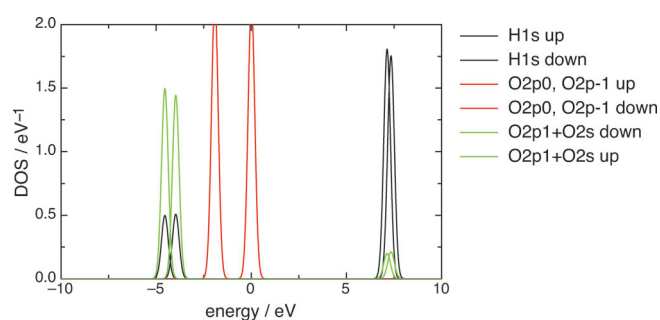
Figure 1. Electronic density of states (DOS) of an OH radical in vacuum. Here and elsewhere, the Fermi level of platinum has been taken as the energy zero.

The adsorption of OH on Pt(111) has been investigated by a number of groups (see refs. [3,4,6] and further references therein). In previous work,[3] we have investigated the electronic interaction with the metal of the different orbitals when the OH is adsorbed on the Pt(111) surface. Herein, we are interested in the electronic interaction as the OH approaches the Pt(111) surface, and its effect on the kinetics of the adsorption. In the optimum geometry the axis of the radical is parallel to the surface. Of the two free p orbitals the p$_0$ orbital is directed towards the surface, whereas the p$_{-1}$ orbital is parallel. As may be expected, the former interacts strongly with the surface, the latter weakly.[3]

When the radical approaches the surface closer than 3.5 Å, spin polarization is lifted. Figure 2 shows the density of states (DOS) of the O2p$_0$ orbital at various distances, and for comparison the sp and d bands of Pt(111) in the absence of adsorption. The DOS of the orbital becomes broader as its distance to the surface decreases, and at short separations one notices the appearance of bonding and antibonding peaks caused by the strong interaction with the d band.[3]

For our theory we require the interaction of the O2p$_0$ orbital with the d and sp bands of platinum. In our previous work on hydrogen evolution[14] we fitted the DOS of the reactant to our theory by assuming that the interaction of a reactant's orbital with a metal band is characterized by a single coupling constant that is independent of energy. However, in the present case it is not possible to obtain satisfactory fits with a constant coupling. We therefore resorted to an idea advanced by Gadzuk et al.[16] in an early work: the interaction depends on the overlap of the orbital with the d and sp states. Metal states with low energies have a shorter range, so that the coupling should increase exponentially with the energy. We have therefore assumed a coupling of the form [Eq. (1)]:

$$V(\varepsilon) = \begin{cases} V_i^0 \exp(\alpha\varepsilon) & \text{for} \quad \varepsilon \leq \varepsilon_c \\ V_i^0 \exp(\alpha\varepsilon_c) & \text{for} \quad \varepsilon \geq \varepsilon_c \end{cases} \tag{1}$$

for both bands; the index i stands for either the d or sp band. A coefficient of $\alpha = 0.5$ proved to give good results. The cutoff energy ε_c is introduced to avoid artifacts appearing at high energies. Its exact value is not important, as long as it is higher than the upper edge of the d band. We have taken $\varepsilon_c = 2$ eV.

As an example, Figure 3 shows the DOS of the O2p$_0$ orbital at a distance of 2.6 Å, and two different fits. Clearly, the fit with an energy-dependent coupling is much better; in particular it fits the peak near 0.2 eV well. The constants V_d^0 and V_{sp}^0 depend roughly exponentially on the distance (see right side of Figure 3). As sp orbitals are more extended than d orbitals, their decay distance is longer. However, at shorter distances the coupling to the d band dominates. Note that these cou-
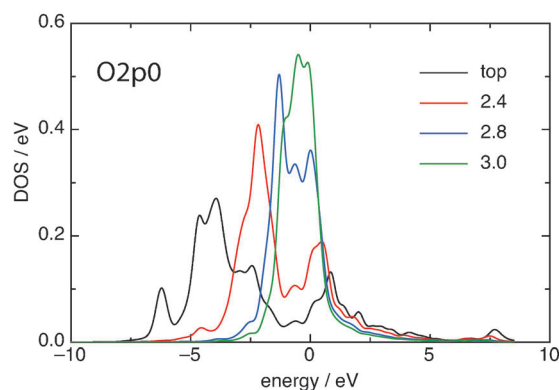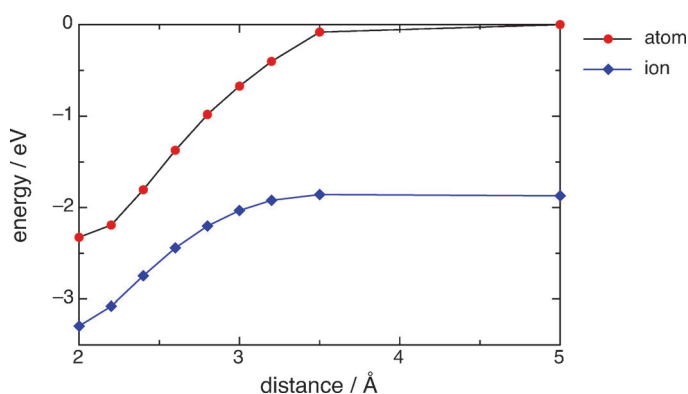

Figure 2. Electronic DOS of pure Pt(111) (left) and of the O2p$_0$ orbital at various distances from the surface (right). The adsorbed state labeled top corresponds to a distance of 2 Å.
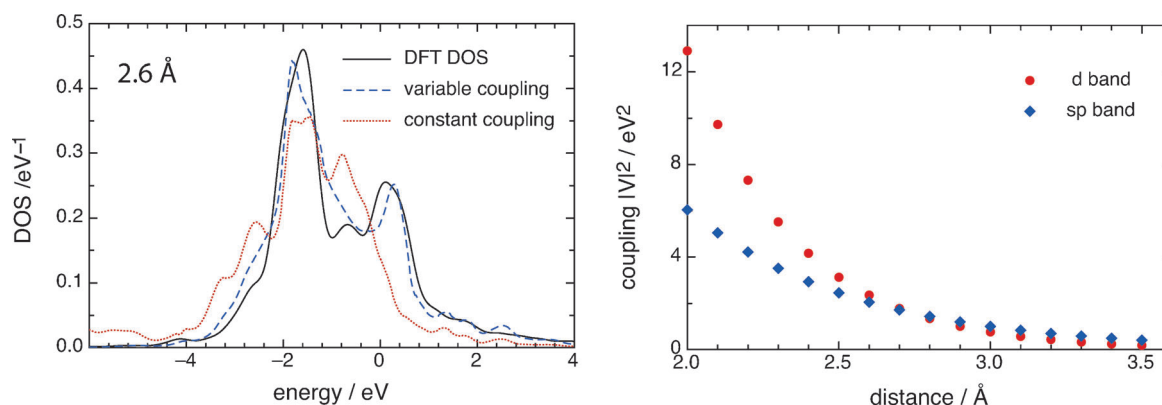
Figure 3. Left: DOS of the $O\,2p_0$ orbital at a distance of 2.6 Å, and corresponding fits with a constant coupling and with an energy-dependent coupling according to Equation (1). Right: coupling constants as a function of the distance.

pling constants cannot be compared with those obtained in previous works with an energy-independent fit.

The initial state in the reaction is the anion OH⁻. The electronic properties of ions are not directly accessible with a DFT code in the slab geometry. As discussed in ref. [15], the most practical way to obtain the electronic properties of ions is to use a localized basis set and apply a high electric field, so that the valence level lies below the Fermi level and is filled. Naturally, one then has to correct the energies for the presence of the field. This we have done to obtain the energy of the anion with respect to the radical; the procedure is described in ref. [15] and a few details are given in the Computational Details. This method gives only relative values, so the energies for the ions have been adjusted such that they reproduce the correct electron affinity at large distances. The results are shown in Figure 4; the energies of both the radical and the ion decrease as they approach the surface. The variation is larger for the radical, which forms a strong chemical bond with the surface. The difference between the value at large distances, set to zero for the radical OH in our normalization, and the adsorbed state at about 2 Å from the surface is the energy of adsorption from the vacuum. Our value of −2.3 eV, obtained for a coverage of 1/9, corresponds quite well to the values obtained by Mavrikakis et al.[17] and Michaelides and Hu.[18] The

low coverage implies that our calculations refer to incipient adsorption.

3. Solvation of OH⁻ near the Electrode Surface

As in all electrochemical reactions, the solvent plays an essential part both in the thermodynamics and in the kinetics of hydroxyl adsorption. The anion is stable, because it is strongly solvated, with a hydration energy of about 4.86 eV.[19] The final state is an adsorbed OH, which is only very weakly solvated; the hydration energy of the OH radical in the bulk of water is only 0.42 eV.[20] In accord with the theories of Marcus,[7] Hush[8] and the Soviet school,[9] the electron transfer to the electrode requires a reorganization of the solvent, which has a large effect on the activation energy for the reaction. Therefore, it is important to have a good description of the solvation of the reactant at the interface.
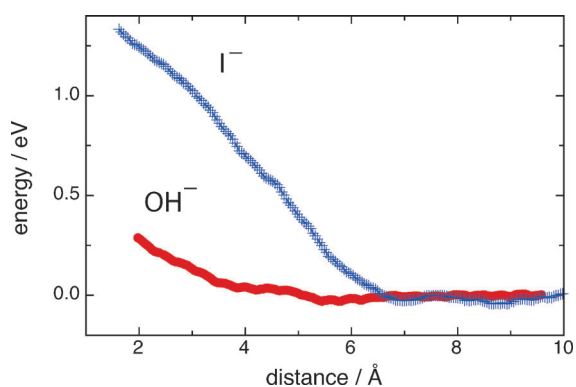
The interaction of an ion with the solvent can be split into two parts: the fast, electronic part, which follows the charge distribution in the system almost instantaneously, and the slow part caused by the dipole orientation. Electron transfer is triggered by fluctuations of the slow part, which must assume an intermediate state between initial and final states. Both parts contribute equally to the free energy of solvation ΔG_{sol}, which does not depend on the solvent kinetics. Following Marcus theory, we base the separation of the total energy of hydration into the slow parts λ_s and the fast part λ_f on the Pekar factor [Eq. (2)]:[21]

$$\lambda_s = \frac{1}{2}\left(\frac{1}{\varepsilon_\infty} - \frac{1}{\varepsilon_s}\right)\Delta G_{sol} \qquad \lambda_f = \frac{1}{2}\left(1 - \frac{1}{\varepsilon_\infty}\right)\Delta G_{sol} \qquad (2)$$

in which ε_∞ is the optical and ε_s the static dielectric constant. For water, $\varepsilon_\infty \approx 1.77$; in the bulk, $\varepsilon_s \approx 80$, but on the surface it is probably somewhat smaller. Therefore, the Pekar factor, which determines the contribution of the slow modes, is about $1/2$, so that both parts contribute about equally to the total energy of hydration. As both parts enter into the free energy surface—the fast modes into the work term, the slow modes into the

Figure 4. Electronic energies of the OH radical and the anion OH⁻ as a function of the distance.

energy of reorganization—a small change in the division between the two kinds of modes has little effect.

Equation (2) provides useful estimates for λ_s and λ_f in the bulk of the solution, but as the ion approaches the electrode, its environment changes, and so does its hydration energy. To calculate this change, we performed classical molecular dynamics simulations and obtained the potential of mean force (PMF) for the approach of the ion towards the surface—the details are given in the Computational Details. As we have discussed before,[12, 13] the PMF depends strongly on how well the ion fits into the structure of water at the surface. Small ions that fit well, such as Ag^+, Cu^+, and OH^-, lose only a small fraction of their hydration energy when they approach the electrode (see Figure 5). For comparison, we also show the PMF for I^- in front of Pt(100), where the PMF rises rapidly, and the ion loses almost half of its hydration energy.[22] In contrast, the PMF for OH^- rises only by 0.3 eV, which is a minor barrier. The sum of the PMF and the solvation energy in the bulk gives the


Figure 5. Potentials of mean force for the approach of OH^- towards Pt(111) and I^- to Pt(100) in aqueous solutions; the potential reflects only the interaction with the solvent, not with the electrode.

solvation energy as a function of position, from which λ_f and λ_s can be calculated.

4. Free Energy Surface for the Reaction

With the electronic energies and the interaction parameters we have the ingredients required to calculate the free energy surface for the reaction. One of the advantages of our method is that we can perform calculations for specific electrode potentials, and we have chosen the equilibrium potential for the overall reaction, which with our unit cells corresponds to equilibrium with a coverage of 1/9. Figure 6 shows the corresponding free energy surface as a function of the distance d from the electrode surface, and of the solvent coordinate q. The latter characterizes the state of the solvent; in our normalization a solvent coordinate of q signifies that the solvent configuration would be in equilibrium with a charge of $-q$ on the reactant. The initial state of our reaction is an OH^- anion with $q = 1$ at large distances. Our calculations cover distances up to 3.5 Å, which is the range at which spin polarization does not occur. The final state is an adsorbed OH on the surface with $q = 0$. Both the initial and the final states show up as absolute minima; in addition there is a local, unstable minimum close to the surface and near $q = 0.8$, which is caused mainly by the image interaction that attracts the ion towards the metal surface. Initial and final states are connected by a ridge with a saddle point near $d = 2.8$ Å and $q = 0.9$ with an energy of activation of about 0.58 eV, which indicates a fast reaction. In comparison, for silver deposition, which is one of the fastest electrochemical reactions, Gerischer observed the same free energy of activation.[35] In the two limits $q = 0$ and $q = 1$ the electronic energies coincide with those obtained by DFT and presented in Figure 4.

The right-hand side of Figure 6 shows the sum of the occupancies of the two orbitals that participate in the reaction: $O\,2p_0$ and $O\,2p_{-1}$. Even though only the former interacts
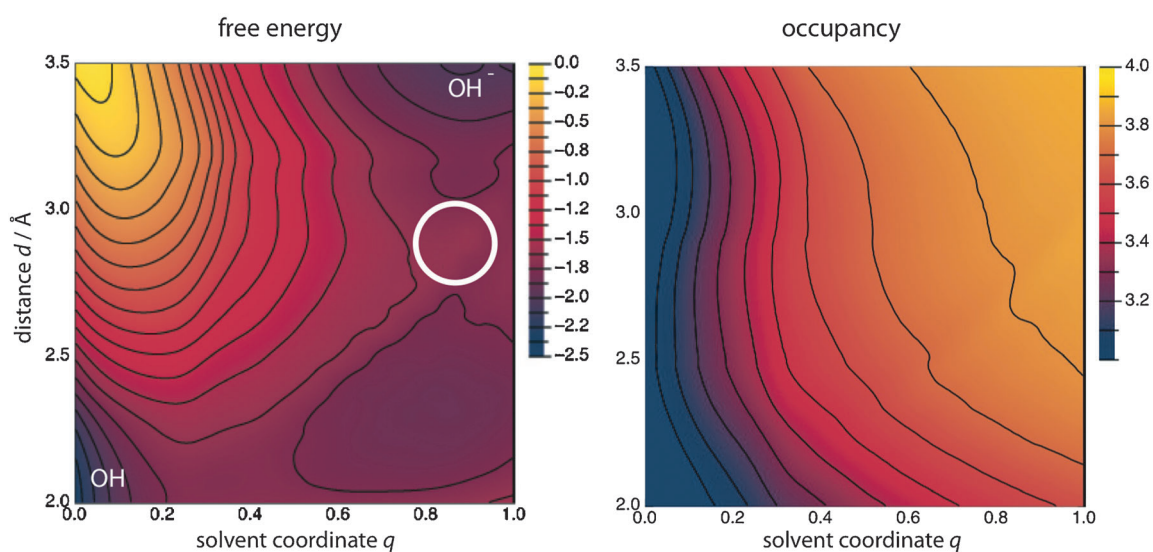

Figure 6. Free energy (left) and total occupancy (right) of the $O\,2p_0$ and $O\,2p_{-1}$ orbitals as a function of the distance and the solvent coordinate. The white circle indicates the saddle point.

strongly with the surface, the participation of the other is important because it takes up half an electron. The total occupation passes smoothly from a value of four for the anion to three for the adsorbate.

In a previous publication[10] we presented preliminary calculations for the same reaction to demonstrate that our theory can be applied to other reactions besides hydrogen evolution. At that time molecular dynamics simulation for OH⁻ did not exist, so we assumed a simple variation of the PMF similar to that observed for I⁻, which resulted in a decrease of the energy of reorganization as the reactant approaches the electrode. Therefore, in that work we obtained a somewhat lower energy of activation. The new value of the activation energy, based on molecular dynamics simulations, should be more reliable than the old one.

The potential dependence of electrochemical reactions is always of special interest. It is sometimes suggested that adsorbed OH plays a role as a short-lived intermediate at a potential lower than the equilibrium value. We have therefore calculated the reaction surface for the case in which the reaction is endergonic by 0.4 V. The saddle point has now shifted towards the surface (see Figure 7), and corresponds to the transition between a physisorbed OH⁻ anion and the adsorbed OH. As the saddle point lies close to the surface, the transfer coefficient is almost unity, and the corresponding activation energy 0.95 eV. This indicates that in the endergonic region OH adsorption is highly unfavorable.
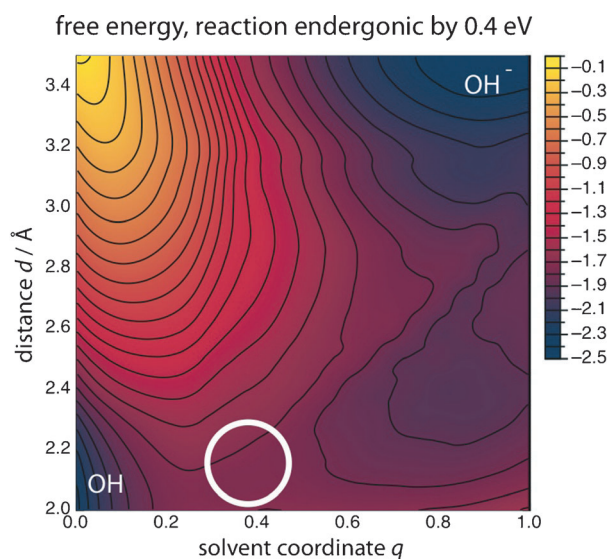
Figure 7. Free energy when the reaction is endergonic by 0.4 eV; the saddle point (white circle) corresponds to an activation energy of 0.95 eV.

It is sometimes suggested that OH adsorption at steps occurs at potentials significantly lower than on terraces, and that it plays a role in reactions that occur in this potential region (for a discussion of this idea, see ref. [36]). We have therefore investigated OH adsorption at a Pt(311) step, but even though the orientation of the adsorbed OH is quite different at the step (see Figure 8), within the usual DFT error the
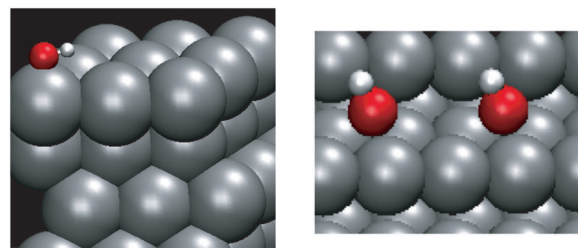
Figure 8. Adsorption of OH at a Pt(111) terrace (left) and at the step of a Pt(311) surface.

adsorption energy is the same as on the terrace. In addition to the site shown in Figure 8, we also investigated the site above the step, and obtained the same result. These findings are somewhat surprising; they are, however, in line with a recent article by van der Niet et al.,[37] who did not find any evidence for a stronger OH adsorption on steps than on terraces. It also explains why the presence of steps does not introduce any new features into the cyclic voltammogram of Pt(111) that can be linked to OH adsorption.[38] Of course, there are other step geometries than the one we have investigated, and we cannot rule out that there are step sites where OH adsorption is stronger than on the terrace.

5. Conclusions

OH adsorption is clearly visible in the cyclic voltammogram of many metals, and plays an important role in oxygen reduction and many other reactions. It has therefore been the subject of numerous studies, both experimental and theoretical. In our work, we have focused on the theory of the kinetics of this reaction on Pt(111) in alkaline solutions, which, with the exception of our own preliminary work, has not been investigated previously. At the same time we improved our theoretical methods significantly by calculating the interaction of the reactant with water through molecular dynamics. In addition, we developed a better procedure to obtain the interaction between the reactant and the electrode as a function of the distance; we now allow for an energy dependence of the coupling constants, and obtain the interaction with both the d and sp bands. These technical advances parallel our recent work on metal deposition.[12, 13]

Still, there are several features of OH adsorption that are badly understood. For example, it is still a mystery why OH adsorption on Pt(111) in alkaline solution gives rise to a broad, featureless peak in the cyclic voltammogram, whereas in acid solutions there is a sharp spike. Another point is a possible hydrogen bonding of the adsorbed OH with an adjacent water molecule, which has been suggested on the basis of DFT calculations,[4, 23] and which we have not considered here.

Concerning our own work, we believe that we have taken a good first step in understanding the kinetics of OH adsorption from alkaline solutions. Our theoretical framework allows for various improvements, such as better interaction potential for the molecular dynamics, or the incorporation of hydrogen bonding of the adsorbed OH with water, if this should prove

to be important. Of special interest should be the application of our model to other metals, to elucidate the catalytic effects on this reaction.

Computational Details

Molecular Dynamics Simulations

Conventional molecular dynamics simulations were performed using the LAMMPS code.[24] To model the system we used a Pt(111) slab with three metal layers (4.62 Å thickness), an ensemble of 469 water molecules, and one OH^- ion initially located in the bulk of the water. The dimensions of the box were $22.63 \times 19.60 \times 36.35$ Å^3. Simulations were carried out at 298 K using the NVT canonical ensemble and a pppm/cg solver was used for corrections to the electrostatic long-range interactions.

The parameters for the interactions between the water molecules in the bulk and between the hydroxide ion and the water were specified by well-known Lennard–Jones potentials. For the water, we used the SPC/E model and the corresponding parameters for the oxygen and hydrogen have been taken from Yoshida et al.[25] The parameters for OH^-–O interaction have been taken from Vácha et al.[26] The interactions between the water molecules and the platinum surface have been obtained by fitting the parameters in Equation (3):

$$V(r) = D_0 \left[e^{(-2\alpha(r-r_0))} - 2e^{(-\alpha(r-r_0))} \right] f_0(\rho) + R_0 e^{(-\beta(r-r_0))} (1 - f_0(\rho)) \quad (3)$$

in which [Eq. (4)]

$$f_0(\rho) = e^{(-\gamma \rho^2)} \text{ with } \rho = \sqrt{\Delta x^2 + \Delta y^2} \quad (4)$$

The parameters used during the simulations for the Pt(111)–water interaction potential are summarized in Table 1.

To calculate the potential of mean force we performed a series of umbrella sampling simulations and analyzed the data using the weighted histogram analysis method (WHAM) code developed by Grossfield.[27] For these simulations we first carried out an equilibration run of 500 ps and then each sample from a total of 21 samples ran for 200 ps, with a time step of 2.0 fs.

Technicalities of the DFT Calculations

The SIESTA code[28] was used to carry out the calculations using

Table 1. Parameters of the potential energy function for the Pt–water interaction.

	D_0 [eV]	α [Å^{-1}]	r_0 [Å]	R_0 [eV]	β [Å^{-1}]	γ [Å^{-1}]
Pt–O	0.4566	1.4961	1.9251	2.6704	3.0838	0.5022
Pt–H	0.0022	1.9258	3.2376	0.0	0.0	0.0

the generalized gradient approximation in the version of Perdew et al.[29] with spin polarization. The ion cores were described by nonconserving nonrelativistic pseudopotentials[30] and a double-ζ plus polarization basis of localized orbitals was used to expand the wavefunctions. All calculations were performed with an energy cutoff of 300 Ry and a k-point mesh of $4 \times 4 \times 1$ in the Monkhorst–Pack scheme.[31] The energy accuracy was reached when the change in the absolute energy value was less than 10 meV, and for

geometry optimization the convergence criterion was achieved when the force on each atom was less than 0.04 eV Å^{-1}.

A (111) platinum surface was modeled by a (3×3) supercell with four metal layers. In all the calculations ten layers of vacuum were considered. For the relaxations, the two bottom layers were fixed at the calculated next-neighbor distance corresponding to bulk, and all the other layers were allowed to relax. The optimized surface—prerelaxed Pt(111)—in the absence of OH was used as input data to carry out the calculations. For the adsorption to take place, the OH radical was located on a top site of the bare Pt(111) according to site stabilities. A coverage of 1/9 was considered in all the calculations. Less OH–Pt coordination and larger OH–metal distances minimize the repulsive interaction and favor the adsorption process given the following adsorption energies: 1) top (−2.62 eV), 2) bridge (−2.28 eV), 3) hollow (−2.57 eV), in agreement with values in the literature.[18, 32, 33] The prerelaxed surfaces were kept fixed while the H in the OH radical was fully relaxed. The O was frozen in all the coordinates at different z distances perpendicular to the surface. The optimized geometry at final equilibrium (OH$_{ads}$ almost flat parallel to the surface) is also in accordance with literature data.[34]

The calculations for the OH^- ion were performed with the SIESTA code as well. This program offers the possibility to add an extra electron to the system; the negative excess charge is then compensated by a constant positive background charge. However, simply adding an electron does not produce an ion, but a negatively charged metal slab. To localize the extra electron on OH, we applied an electric field, which was sufficient to shift the affinity level of OH below the Fermi level of platinum; a field of 2 V Å^{-1} proved to be sufficient. Keeping this field constant, we calculated the energy of the ions as a function of the distance, in the range of 2 to 4.6 Å. To obtain absolute values, the resulting energies have to be corrected for four effects: 1) the effect of the field, 2) the effect of background charge on the energy of the ion, 3) the self-interaction of the background charge, and 4) the interaction energy of the slab with the background[9] and the field. The first two terms are easily calculated; the latter two are independent of the position of the ion, as long as it does not form a chemical bond with the metal, which is true in the range investigated. The latter two terms are difficult to calculate for numerical reasons and were not evaluated. Instead, the energy of the ion, corrected for the first two effects, was adjusted by adding a constant in such a way that at large distances it reproduces the experimental electron affinity of the radical.

[1] N. Ramaswamy, S. Mukerjee, *Adv. Phys. Chem.* **2012**, 491604.

[2] D. Strmcnik, M. Uchimura, C. Wang, R. Subbaraman, N. Danilovic, D. van der Vliet, A. P. Paulikas, V. R. Stamenkovic, N. Markovic, *Nat. Chem.* **2013**, *5*, 300.

[3] M. D. Arce, P. Quaino, E. Santos, *Catal. Today* **2013**, *202*, 120.

[4] J. Rossmeisl, J. K. Nørskov, C. D. Taylor, M. J. Janik, M. Neurock, *J. Phys. Chem. B* **2006**, *110*, 21833.

[5] A. Hodgson, S. Haq, *Surf. Sci. Rep.* **2009**, *64*, 381.

[6] C. D. Taylor, R. G. Kelly, M. Neurock, *J. Electrochem. Soc.* **2007**, *154*, F217.

[7] R. A. Marcus, *J. Chem. Phys.* **1956**, *24*, 966.

[8] N. S. Hush, *J. Chem. Phys.* **1958**, *28*, 962.

[9] A. M. Kuznetsov, *Charge Transfer in Physics, Chemistry and Biology*, Gordon and Breach, Reading, **1995**, p. 622.

[10] E. Santos, A. Lundin, K. Pötting, P. Quaino, W. Schmickler, *Phys. Rev. B* **2009**, *79*, 235436.

[11] P. Quaino, N. B. Luque, R. Nazmutdinov, E. Santos, W. Schmickler, *Angew. Chem. Int. Ed.* **2012**, *51*, 12997; *Angew. Chem.* **2012**, *124*, 13171.

[12] L. M. C. Pinto, E. Spohr, P. Quaino, E. Santos, W. Schmickler, *Angew. Chem. Int. Ed.* **2013**, *52*, 7883; *Angew. Chem.* **2013**, *125*, 8037.

[13] L. M. C. Pinto, P. Quaino, E. Santos, W. Schmickler, *ChemPhysChem* **2014**, *15*, 132.

[14] E. Santos, P. Quaino, W. Schmickler, *Phys. Chem. Chem. Phys.* **2012**, *14*, 11224.

[15] P. Quaino, N. Luque, G. Soldano, R. Nazmutdinov, E. Santos, T. Roman, A. Lundin, A. Groß, W. Schmickler, *Electrochim. Acta* **2013**, *105*, 248.

[16] J. W. Gadzuk, J. K. Hartmann, T. N. Rhodin, *Phys. Rev. B* **1971**, *4*, 241.

[17] D. C. Ford, Y. Xu, M. Mavrikakis, *Surf. Sci.* **2005**, *587*, 159.

[18] A. Michaelides, P. Hu, *J. Chem. Phys.* **2001**, *114*, 513.

[19] *Standard Potentials in Aqueous Solutions* (Eds.: A. Bard, R. Parsons, J. Jordan), Marcel Dekker, New York, **1985**, p. 834.

[20] G. V. Buxton, C. L. Greenstock, W. P. Helman, A. K. Ross, *J. Phys. Chem. Ref. Data* **1988**, *17*, 513.

[21] a) S. I. Pekar, *Untersuchungen über die Elektronentheorie der Kristalle*, Akademie-Verlag, Berlin, **1954**, p. 184; b) S. I. Pekar, *Research in Electron Theory of Crystals*, United States Atomic Energy Commission, Washington D.C., **1963**, p. 240.

[22] O. Pecina, W. Schmickler, E. Spohr, *J. Electroanal. Chem.* **1995**, *394*, 29.

[23] P. Vassilev, M. T. M. Koper, R. A. van Santen, *Chem. Phys. Lett.* **2002**, *359*, 337.

[24] S. Plimpton, *J. Comput. Phys.* **1995**, *117*, 1.

[25] K. Yoshida, T. Yamaguchi, A. Kovalenko, F. Hirata, *J. Phys. Chem. B* **2002**, *106*, 5042.

[26] R. Vácha, T. Megyes, I. Bakó, L. Pusztai, P. Jungwirth, *J. Phys. Chem. A* **2009**, *113*, 4022.

[27] A. Grossfield, "WHAM: an implementation of the weighted histogram analysis method", version 2.0.6, can be found under http://membrane.urmc.rochester.edu/content/wham.

[28] J. M. Soler, E. Artacho, J. D. Gale, A. García, J. Junquera, P. Ordejón, D. Sánchez-Portal, *J. Phys. Condens. Matter* **2002**, *14*, 2745.

[29] J. P. Perdew, K. Burke, M. Ernzerhof, *Phys. Rev. Lett.* **1996**, *77*, 3865.

[30] N. Troullier, J. L. Martins, *Phys. Rev. B* **1991**, *43*, 1993.

[31] H. J. Monkhorst, J. D. Pack, *Phys. Rev. B* **1976**, *13*, 5188.

[32] G. S. Karlberg, *Phys. Rev. B* **2006**, *74*, 153414.

[33] A. B. Anderson, N. M. Neshev, R. A. Sidik, P. Shiller, *Electrochim. Acta* **2002**, *47*, 2999.

[34] A. P. Seitsonen, Y. Zhu, K. Bedürftig, H. Over, *J. Am. Chem. Soc.* **2001**, *123*, 7347.

[35] H. Gerischer, *Z. Elektrochem.* **1958**, *62*, 256.

[36] M. T. M. Koper, S. C. S. Lai, E. Herrero in *Fuel Cell Catalysis: A Surface Science Approach* (Ed.: M. T. M. Koper), Wiley, Hoboken, **2009**, pp. 159–208.

[37] M. J. T. C. van der Niet, A. den Dunnen, L. B. F. Juurlink, M. T. M. Koper, *Angew. Chem. Int. Ed.* **2010**, *49*, 6572; *Angew. Chem.* **2010**, *122*, 6772.

[38] M. J. T. C. van der Niet, N. Garcia-Araez, J. Hernández, J. M. Feliu, M. T. M. Koper, *Catal. Today* **2013**, *202*, 105.